ISSN 1063-7761, Journal of Experimental and Theoretical Physics, 2008, Vol. 106, No. 4, pp. 765–772. © Pleiades Publishing, Inc., 2008.
Original Russian Text © S.S. Aplesnin, L.I. Ryabinkina, O.B. Romanova, D.A. Velikanov, A.D. Balaev, D.A. Balaev, K.I. Yanushkevich, A.I. Galyas, O.F. Demidenko, O.N. Bandurina, 2008, published in Zhurnal Éksperimental'noĭ i Teoreticheskoĭ Fiziki, 2008, Vol. 133, No. 4, pp. 875–883.

NUCLEI, PARTICLES, FIELDS, GRAVITATION, AND ASTROPHYSICS

Transport Properties and Ferromagnetism of $Co_xMn_{1-x}S$ Sulfides

S. S. Aplesnin[a,b], L. I. Ryabinkina[a], O. B. Romanova[a,*], D. A. Velikanov[a], A. D. Balaev[a], D. A. Balaev[a], K. I. Yanushkevich[c], A. I. Galyas[c], O. F. Demidenko[c], and O. N. Bandurina[b]

[a] *Kirensky Institute of Physics, Siberian Branch, Russian Academy of Sciences, Krasnoyarsk, 660036 Russia*

[b] *Reshetnev Siberian State Aerospace University, Krasnoyarsk, 660014 Russia*

[c] *Joint Institute of Solid State and Semiconductor Physics, National Academy of Sciences of Belarus, Minsk, 220072 Belarus*

e-mail: rob@iph.krasn.ru

Received July 6, 2007

Abstract—We have studied the resistivity and thermoelectromotive force (thermo emf) in a temperature range of $T = 80$–1000 K, the magnetic susceptibility and magnetization in a temperature range of $T = 4.2$–300 K at an external magnetic field of up to 70 kOe, and the structural characteristics of $Co_xMn_{1-x}S$ sulfides ($0 \le x \le 0.4$). Anomalies in the transport properties of these compounds have been found in the temperature intervals $\Delta T_1 = 200$–270 K and $\Delta T_2 = 530$–670 K and at $T_3 \sim T_N$. The temperature dependences of the magnetic susceptibility, magnetization, and resistivity, as well as the current–voltage characteristics, exhibit hysteresis. In the domain of magnetic ordering at temperatures below the Néel temperature (T_N), the antiferromagnetic $Co_xMn_{1-x}S$ sulfides possess a spontaneous magnetic moment that is explained using a model of the orbital ordering of electrons in the t_{2g} bands. The influence of the cobalt-ion-induced charge ordering on the transport and magnetic properties of sulfides has been studied. The calculated values of the temperatures corresponding to the maxima of charge susceptibility, which are related to a competition between the on-site Coulomb interaction of holes in various subbands and their weak hybridization, agree well with the experimental data.

PACS numbers: 71.20.Nr, 71.27.+a, 73.43.Cd, 73.20.Fz, 73.50.Lw

DOI: 10.1134/S1063776108040158

1. INTRODUCTION

In recent years, a new direction of research and technology called spintronics has been extensively developed [1–3], which combines the advantages of energy-independent magnetic memory devices and high-speed electric data processing systems. The transformations of electric signals in spintronics are performed using both the charge state of electrons and their spin states, which make possible the creation of important new spintronic devices such as high-speed RAM in computers, novel sensors, magnetic-to-optical signal converters, etc. In connection with this, much attention has been devoted to the creation and characterization of new magnetic materials, which combine useful magnetic, electrical, and optical properties related to features of the composition-dependent crystalline order and the electron energy band structure. This class of substances includes disordered systems, in which metal–insulator transition (MIT) and the phenomenon of colossal magnetoresistance (CMR) are observed [4–8]. Various groups of compounds featuring MIT and CMR phenomena have been extensively studied, including manganese oxides (e.g., $LaMnO_3$ type manganites) [8–12], europium chalcogenides [13], selenides ($CdCr_2Se_4$ and $HgCr_2Se_4$) and sulfides [14–19].

Cation-substituted sulfides of the $Me_xMn_{1-x}S$ systems (Me = Cr, Fe) are also known to exhibit the MIT and show a CMR whose magnitude is comparable to that in manganites [20–25]. Monosulfide α-MnS is an antiferromagnet with a Néel temperature of $T_N = 150$ K, which crystallizes in a NaCl-type face-centered cubic (fcc) lattice. The magnetic structure of this compound is characterized by a ferromagnetic ordering of the magnetic moments of manganese ions in the (111) type planes and an antiferromagnetic ordering between these planes [26, 27]. The results of energy-band structure calculations performed for α-MnS using the electron density functional method [28] showed a partial occupation of the upper Hubbard t_{2g} and e_g bands as a result of the p–d hybridization between sulfur and manganese ions. The conductivity due to electron states in the t_{2g} and e_g bands below the Fermi level has a hole character, which is confirmed by the results of the thermo emf and Hall effect measurements [29]. According to our calculations [30] a charge-density wave existing in α-MnS can exhibit pinning when manganese ions are replaced by other transition metal ions capable of sufficiently strong hybridization with sulfur anions. One possible substituent of this kind is a divalent cobalt ion (Co^{2+}) whose t_{2g} shell needs only one

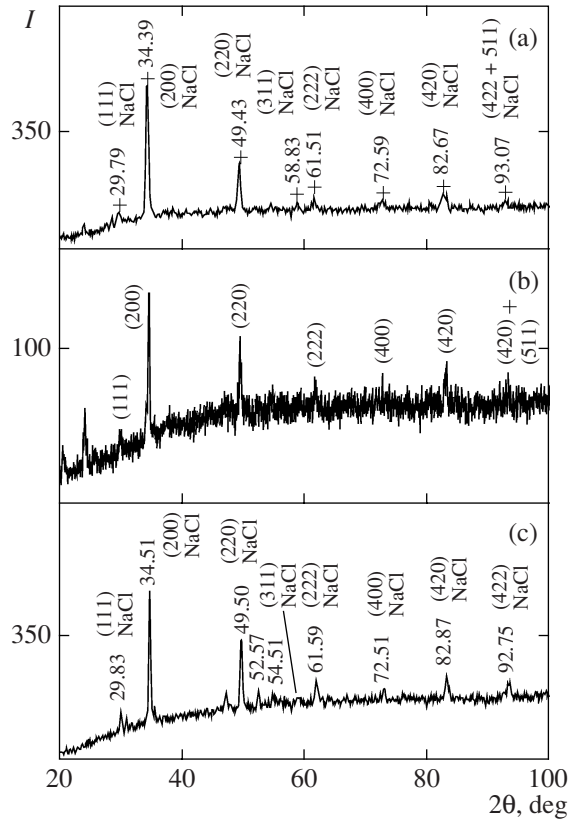

Fig. 1. X-ray diffraction patterns of (a) $Co_{0.2}Mn_{0.8}S$, (b) $Co_{0.3}Mn_{0.7}S$, and (c) $Co_{0.4}Mn_{0.6}S$ measured at $T = 300$ K.

electron to be completely filled, which can be represented as a hole. The triple hole degeneracy in the t_{2g} shell can be removed under the action of a crystal field induced by lattice distortions. By synthesizing solid solutions of the $Me_xMn_{1-x}S$ systems by means of cobalt substitution for manganese and studying their electrical and magnetic properties, it is possible to trace the laws of variation of the conductivity type and magnetic order and open ways to the creation of new materials possessing special combinations of properties, including MIT and CMR [4–8, 31–33].

Using reactions in evacuated quartz ampules, we synthesized solid solutions of the $Co_xMn_{1-x}S$ system ($0 \le x \le 0.4$) with a NaCl-type fcc lattice [34], in agreement with the neutron diffraction data [35], showing evidence for the stability and single-phase character of the fcc structure of $Co_xMn_{1-x}S$ solid solutions. The magnetic properties of the synthesized compounds were studied by the ponderomotive technique in a field of 8.6 kOe at temperatures in the 80–1000 K range [34]. The samples exhibited antiferromagnetic ordering with a Néel temperature increasing from $T_N = 150$ K (for $x = 0$) to $T_N = 196$ K (for $x = 0.4$). The substitution of cobalt for manganese in $Co_xMn_{1-x}S$ leads to a concentration-driven semiconductor–semimetal phase transition at $x_c = 0.4$, involving a change in the type of conductivity [36].

This work was aimed at studying the interrelated magnetic and electrical properties of $Co_xMn_{1-x}S$ sulfides by a combination of theoretical and experimental methods, including a complex study of the crystal structure, resistivity, thermo emf, current–voltage characteristics, magnetic susceptibility, and magnetization in a broad range of temperatures (4.2–1000 K) and magnetic fields (up to 70 kOe). Another goal was to elucidate the mechanism by which the cobalt-ion-induced charge ordering influences the transport and magnetic properties of $Co_xMn_{1-x}S$ sulfides in the magnetically ordered state.

2. EXPERIMENTAL METHODS AND RESULTS

The crystal structure of $Co_xMn_{1-x}S$ sulfides was studied at $T = 300$ K by X-ray diffraction on a DRON-3 diffractometer using monochromated CuK_α radiation. X-ray diffraction measurements were performed on the samples before and after investigation of the temperature dependences of the magnetic susceptibility $\chi(T)$, resistivity $\rho(T)$, and thermo emf $\alpha(T)$.

According to the results of the X-ray structure analysis, the samples of $Co_xMn_{1-x}S$ sulfides with $0 \le x \le 0.4$ possess a NaCl-type fcc lattice, which is also inherent in α-MnS [34, 36]. As the degree of cationic substitution (x) is increased, the lattice parameter exhibits a linear decrease from about 5.222 Å ($x = 0$) to 5.204 Å ($x = 0.4$), which is evidence for the formation of continuous solid solutions based on α-MnS. Figure 1 shows typical X-ray diffraction patterns of various samples.

The resistivity and thermo emf were studied using the conventional direct-current four-point-probe compensation technique in a temperature range of $T = 80$–1000 K in the absence of magnetic field. The temperature dependence of the resistivity was also measured on the samples cooled in a zero electric field and in a field of $E = 140$ V/cm in a temperature range of $T = 4.2$–100 K. The magnetic properties of samples were studied using a SQUID magnetometer in a magnetic field of $H = 0.5$ kOe and using a vibrating-sample magnetometer with a superconducting coil in magnetic fields $H \le 70$ kOe in a temperature range of $T = 4.2$–100 K.

The samples of $Co_xMn_{1-x}S$ sulfides exhibited hysteresis of the magnetization at low temperatures ($T < 50$ K) in a field of 0.5 kOe (Fig. 2). Under these conditions, the magnetization varied by a factor of about $\sigma_{FC}/\sigma_{ZFC} \sim 2$, where σ_{FC} and σ_{ZFC} are the values of magnetization measured on cooling the sample in an applied magnetic field (field cooling, FC) and in the absence of magnetic field (zero field cooling, ZFC), respectively. As can be seen, the composition with $x = 0.05$ is characterized by a quite large magnetization: $\sigma \sim 0.8$ G cm^3/g up to a temperature of 120 K in a field of 0.5 kOe (Fig. 2b).

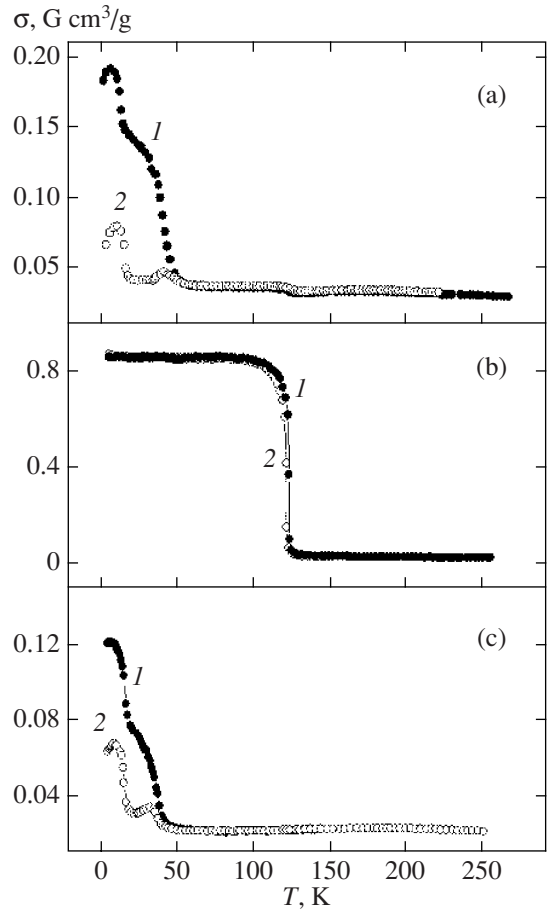

Fig. 2. Temperature dependences of the magnetization of (a) $Co_{0.02}Mn_{0.98}S$, (b) $Co_{0.05}Mn_{0.95}S$, and (c) $Co_{0.3}Mn_{0.7}S$ measured on cooling (*1*) in a magnetic field of $H = 0.5$ kOe (field cooling, FC) ad (*2*) in a zero magnetic field (zero-field cooling, ZFC).

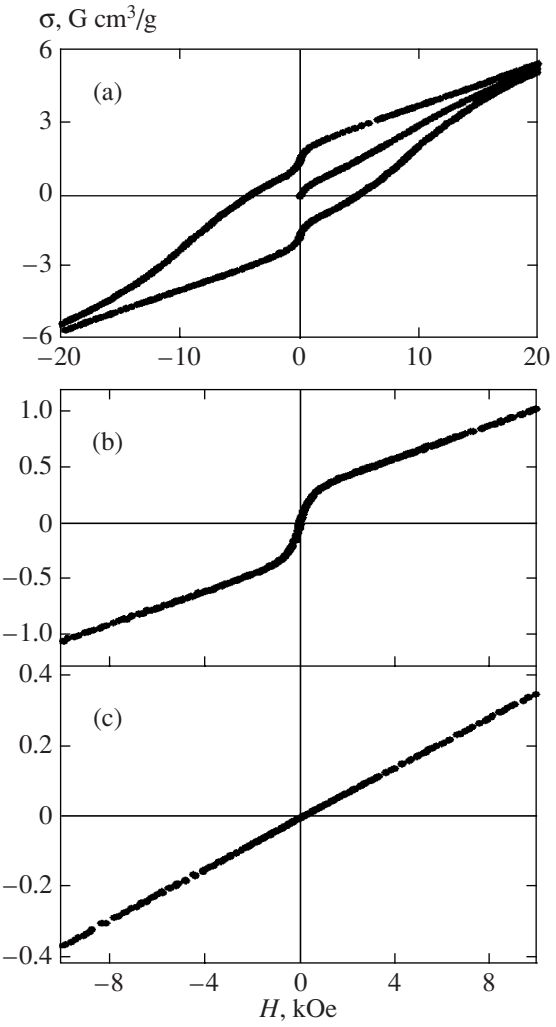

Fig. 3. Hysteresis in the magnetization in $Co_{0.05}Mn_{0.95}S$ at $T = 4.2$ K (a), 115 K (b), and 130 K (c).

In the domain of magnetic ordering (at temperatures $T < T_N$), the antiferromagnetic $Co_xMn_{1-x}S$ solid solution exhibit the formation of a spontaneous magnetic moment. This is confirmed by the presence of hysteresis in the magnetization curve $\sigma(H)$ (Figs. 3 and 4). For a composition with $x = 0.05$, the spontaneous magnetic moment appears at a critical temperature of $T_c < 120$ K (Fig. 3). As the cobalt concentration (x) is increased, the critical temperature (T_c) for the appearance of a spontaneous magnetic moment decreases and attains $T_c \sim 50$ K for $x = 0.3$ (Fig. 4a). The temperature hysteresis of magnetization observed on cooling of this sample both in the ZFC and FC (10 kOe) regimes exhibits correlation with the hysteresis of resistivity measured on heating and cooling of the sample in the zero magnetic field (Fig. 4a).

The measurements of resistivity for $Co_xMn_{1-x}S$ solid solutions were performed in a temperature range of 80–1000 K. The temperature dependences of $\log\rho(10^3/T)$ for the compositions with $x \le 0.3$ are indicative of a semiconductor character of conduction, with a resistivity of $\rho \sim 10^5$ Ω cm ($x = 0.3$) at $T = 80$ K (Fig. 5). The temperature-dependent behavior of the resistivity of these sulfides, plotted as $\log\rho(10^3/T)$, can be approximated by three steps with plateaus in the temperature intervals of $\Delta T_1 \approx 200$–270 K and $\Delta T_2 \approx 530$–670 K and at $T_3 \sim T_N$. In the region of $T = T_N$, the samples with cobalt concentrations $x = 0.02$–0.30 exhibit an insulator–semiconductor anomaly, in which the conductivity activation energy changes, for example, from 0.01 eV (below T_N) to 0.14 eV (above T_N) for $x = 0.3$. In a temperature interval of 80–600 K, these compositions exhibit extrinsic (impurity) conduction, while the region of $T > 600$ K corresponds to the intrinsic conduction (Fig. 5). The bandgap width ΔE determined from the slope of the linear part of the $\log\rho(1/T)$ plot above $T = 600$ K changes from 1.46 eV for α-MnS ($x = 0$) to 0.42 eV for $Co_xMn_{1-x}S$ with $x = 0.3$.

Figure 6 shows the temperature dependences of the thermo emf (Seebeck coefficient) $\alpha(T)$ for various

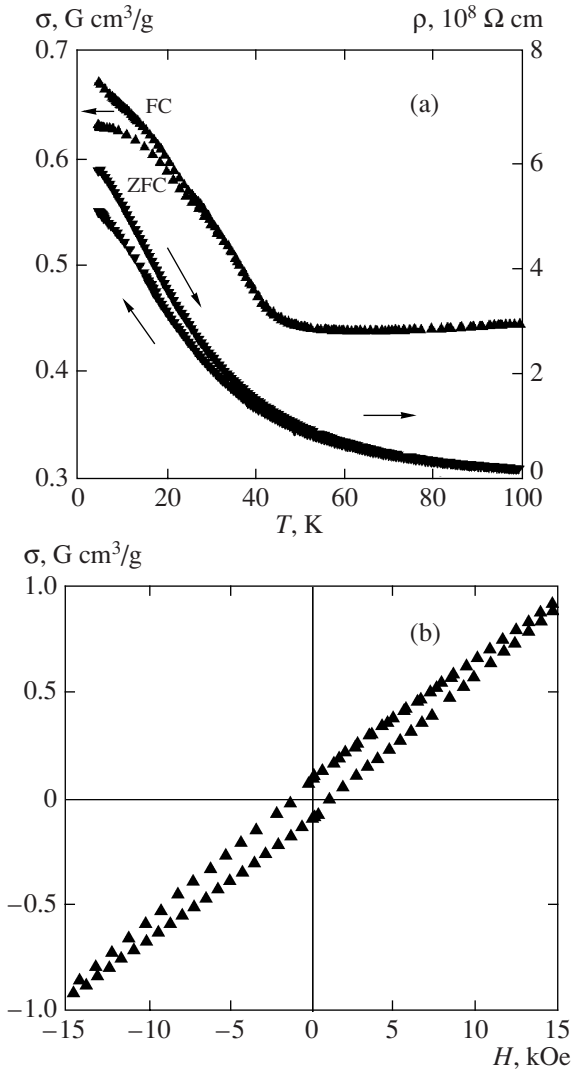

Fig. 4. Hysteresis in the electrical and magnetic properties of $Co_{0.3}Mn_{0.7}S$: (a) Temperature dependences of the magnetization in a field of $H = 10$ kOe measured upon ZFC and FC (left-hand scale) and the resistivity measured at $H = 0$ in the heating and cooling regimes (right-hand scale); (b) isotherms of magnetization at $T = 4.2$ K.

$Co_xMn_{1-x}S$ compounds with $0 \le x \le 0.3$. The $\alpha(T)$ curve obtained for α-MnS (Fig. 6a) coincides with the dependence reported by Heikens et al. [29]. The positive sign $\alpha(T)$ of the thermo emf in this case is indicative of the hole-type conductivity in α-MnS. The thermo emf in $Co_xMn_{1-x}S$ with $0 \le x \le 0.3$ is also positive ($\alpha > 0$) and decreases with increasing cobalt content. Indeed, α reaches 1200 μV/K in $Co_{0.02}Mn_{0.98}S$ at $T = 650$–700 K and decreases below 100 μV/K for $Co_{0.3}Mn_{0.7}S$ in the same temperature interval. The maximum values of α for the compositions with $x = 0.2$–0.3 are observed in the temperature interval of 200–270 K. Further increase in the cobalt content leads to a sharp drop in the thermo emf.

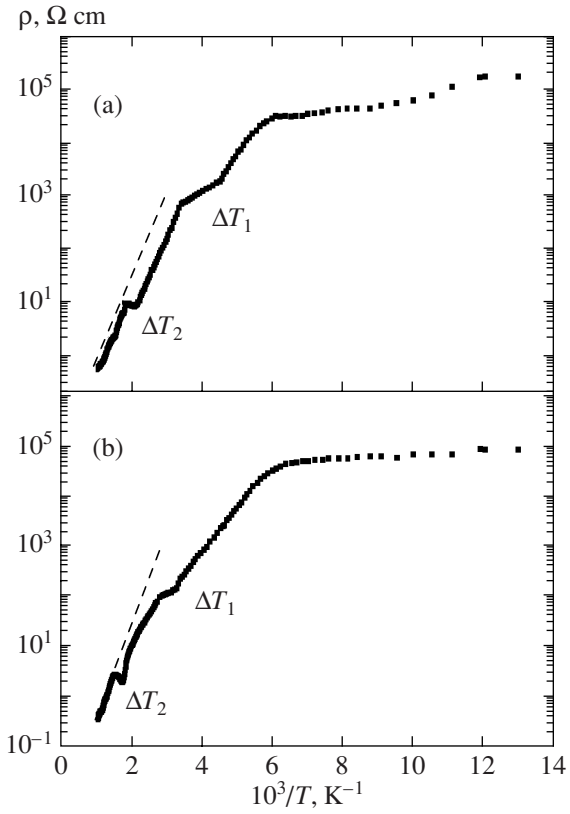

Fig. 5. Temperature dependences of the resistivity for (a) $Co_{0.2}Mn_{0.8}S$ and (b) $Co_{0.3}Mn_{0.7}S$.

Figure 7 shows for $x = 0.3$ the results of resistance measurements in the low-temperature region (4.2–100 K) for a sample initially cooled in a zero electric field and then heated and cooled in a field of $E = 140$ V/cm. As can be seen, the resistance exhibits a hysteresis. It was established that the magnitude of this hysteresis depended on the sample prehistory. Analogous features were also manifested in the current–voltage (I–U) characteristics of these samples. Figure 8 presents the I–U characteristics measured in a zero magnetic field, which show that the curves obtained in the regimes of increasing and decreasing bias voltage do not coincide with each other. The hysteresis virtually disappears at $T \sim 80$ K and in the presence of a strong magnetic field (about 60 kOe).

3. THEORETICAL MODEL

According to the results of X-ray structure analysis, $Co_xMn_{1-x}S$ solid solutions possess a NaCl type cubic crystal symmetry. As the cobalt content is increased to $x = 0.2$, the effective exchange field exhibits a 10% increase, while the resistance decreases by the same amount. The results of the electron density functional calculations [28] showed that α-MnS exhibits redistribution of the electron density as a result of the hybrid-

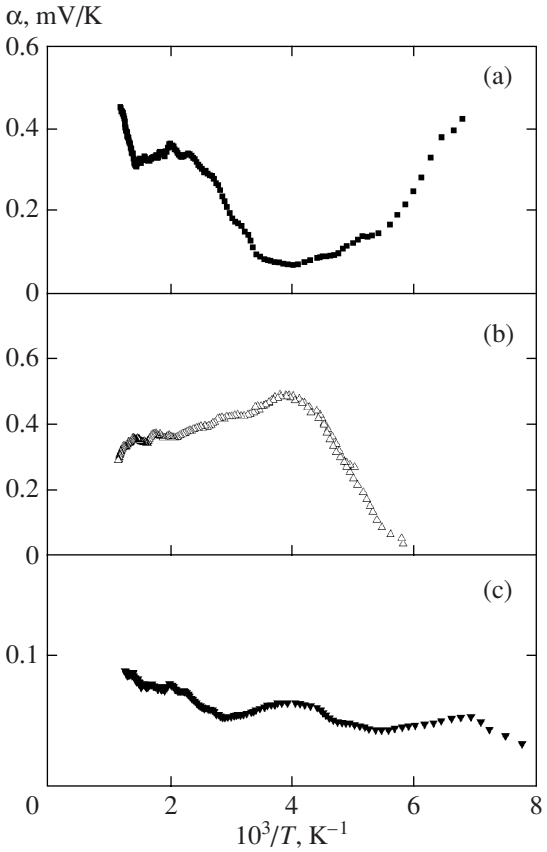

Fig. 6. Temperature dependences of the thermo emf for (a) α-MnS, (b) $Co_{0.2}Mn_{0.8}S$, and (c) $Co_{0.3}Mn_{0.7}S$.

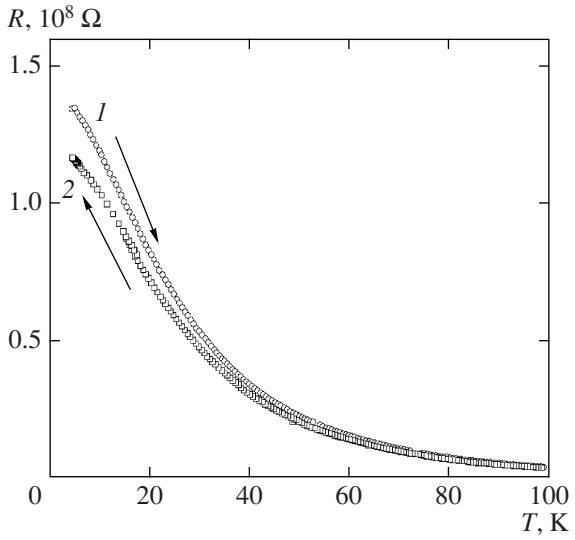

Fig. 7. Temperature dependences of the resistances of $Co_{0.3}Mn_{0.7}S$ initially cooled in the zero electric field and then (*1*) heated and (*2*) cooled in a field of $E = 140$ V/cm.

ization between sulfur and manganese ions. A schematic diagram of the electron density of states was also presented in [28].

Electrostatic interaction of an excess charge removes the double and triple degeneracy of the t_{2g} and e_g bands in the field of cubic symmetry and leads to a local and global breakage of this symmetry. The exchange interaction of electrons on various orbitals is much weaker than the Coulomb interaction between these electrons ($J/U \sim 0.2$) and, hence, can be ignored. Below, we also ignore the hybridization of the t_{2g} and e_g bands caused by a strong crystal field (about 2 eV).

Let us consider the motion of charge carriers only in the upper Hubbard band within the framework of an effective model with spinless fermions. The concentration of carriers in this band is proportional to the content of cobalt ions, which have a single hole in the t_{2g} band in the octahedral environment. In the virtual crystal approximation, the Hamiltonian has the following form:

$$H_t = -\sum_{i,j,\alpha} t_{i,j}^{\alpha\alpha} a_{i\alpha}^{\dagger} a_{j\alpha} - \sum_{i,j,\alpha>\beta} t_{i,j}^{\alpha\beta} a_{i\alpha}^{\dagger} a_{j\beta} - \mu n + \sum_{i,\alpha>\beta} U n_{i\alpha} n_{i\beta},$$

$$H_e = -\sum_{i,j,\alpha} t_{i,j}^{\alpha\alpha} c_{i\alpha}^{\dagger} c_{j\alpha} - \sum_{i,j,\alpha>\beta} t_{i,j}^{\alpha\beta} c_{i\alpha}^{\dagger} c_{j\beta} - \mu n + \sum_{i,\alpha>\beta} U n_{i\alpha} n_{i\beta}, \quad (1)$$

where $a_{i\alpha(\beta)}$ is the operator of electron annihilation in $t_{2g,\,\alpha(\beta)}$ subbands ($\alpha(\beta) = xy, yz, zx$), $c_{i\alpha(\beta)}$ is the operator of electron annihilation in $e_{g,\,\alpha(\beta)}$ subbands ($\alpha(\beta) = x^2 - y^2, 3z^2 - r^2$), μ is the chemical potential, n_i are the on-site hole occupation numbers, and $t_{i,j}^{\alpha\alpha}$ is the hopping integral. Equations for the Green's functions are derived and the excitation spectrum is calculated as described elsewhere [30]. The hopping integral $t_{i,j}^{\alpha\alpha}$ is inversely proportional to the lattice parameter a and can be expressed as $t \propto 1/a^{\gamma}$, where the exponent γ varies according to various estimates within 3–4. As cobalt is substituted for manganese, the change in the lattice parameter amounts to $a_{(x=0.3)}/a_{(x=0)} = 0.997$, while the change in the hopping integral as a result of doping amounts to several percent. For this reason, we ignore the variation of $t_{i,j}^{\alpha\alpha}$ in $Co_xMn_{1-x}S$ solid solutions in comparison to that in α-MnS [30] and take into account only the change in the charge carrier concentration n.

4. DISCUSSION OF EXPERIMENTAL RESULTS

The presence of anomalies in the temperature dependence of the conductivity, which appear as steps

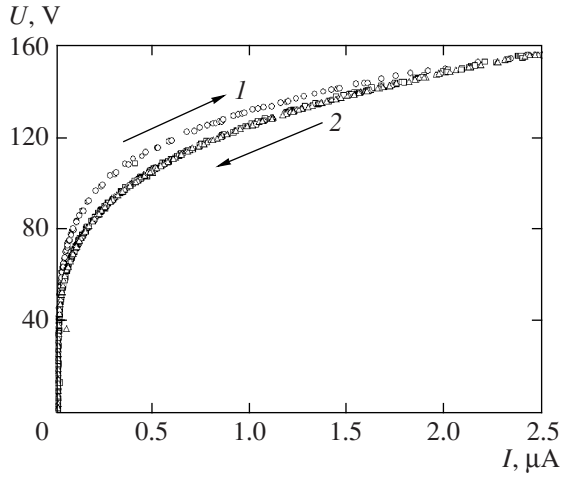

Fig. 8. Current–voltage (I–U) characteristics of $Co_{0.3}Mn_{0.7}S$ measured at $T = 4.2$ K in a zero magnetic field: (*1*) forward branch (bias voltage U increases); (*2*) reverse branch (U decreases); after the first 1–2 cycle, the forward and reverse branches in subsequent cycles coincide with curve *2*.

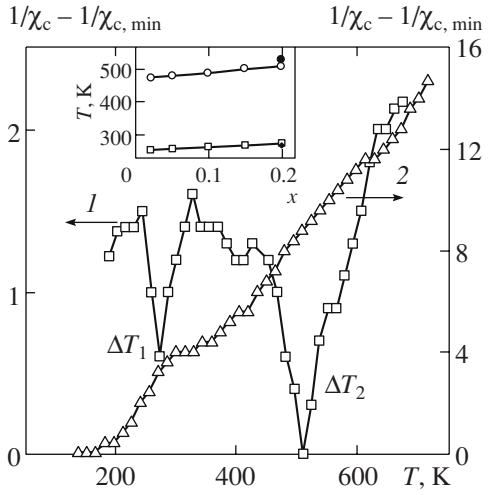

Fig. 9. Temperature dependence of the difference between the inverse charge susceptibility χ_c^{-1} and the minimum inverse susceptibility $\chi_{c,\min}^{-1}$ determined at ΔT_2 for in $Co_xMn_{1-x}S$ ($x = 0.2$) in the (*1*) t_{2g} and (*2*) e_g bands. The inset shows plots of the temperatures (*1*) ΔT_1 and (*2*) ΔT_2 of the maximum charge susceptibility versus cobalt concentration x (empty symbols show theoretical values, solid symbols represent experimental data).

with plateaus in the ΔT_1 and ΔT_2 intervals (Fig. 5), and the maximum of thermo emf in the region of $T \approx 250$–270 K (Fig. 6) correlates with changes in the electron density N_μ at the level of the chemical potential. Calculations of the temperature dependence of N_μ revealed features manifested as a change in the slope dN_μ/dT in the regions of ΔT_1 and ΔT_2, which is analogous to those observed for α-MnS [30]. On heating of a sample, the redistribution of electron density over subbands as a result of the hybridization of d_{xy}, d_{xz}, d_{yz} orbitals leads to changes in the interorbital Coulomb interaction between particles and in the quasi-gap width, which significantly influences the temperature dependence of the conductivity. Calculations of the thermodynamic potential show a change in the occupation numbers n_α ($\alpha = 1, 2, 3$) over d_{xy}, d_{xz}, d_{yz} subbands. Indeed, for $T > \Delta T_2$, the thermodynamic potential exhibits a minimum at $n_1 = n_2 = n_3 = n/3$, while for $T < \Delta T_1$, a minimum is attained at $n_1 = n_2 = 0$, $n_3 = n$.

The charge susceptibility of holes calculated as

$$\chi_c = \frac{dn}{d\mu} = \sum_k \frac{dN(k)}{d\mu} \qquad (2)$$

has two maxima in the t_{2g} band and one maximum in the e_g band (Fig. 9). Theoretical calculations of the charge susceptibility performed for the parameters of the model [30] showed that this quantity has maxima in the temperature intervals $\Delta T_1 = 250$–270 K and $\Delta T_2 = 470$–520 K, which leads to the formation of an orbital magnetic order.

If the nearest environment of a Co^{2+} ion contains only manganese ions, then the difference in the electronegativity of manganese and cobalt ions leads to a change in the electron density at one of the neighboring Mn^{2+} ions, as well as in the length of a covalent Co–S–Mn bond, which is related to the hybridization of orbitals d_{zx}–p_z–d_{zx} and d_{zy}–p_z–d_{zy}. One possible physical mechanism consists in the intraatomic Coulomb repulsion of electrons on the same orbital in the t_{2g} state of Co^{2+}. A change in the Co–Mn distance in the cubic crystal is degenerate with respect to the direction and leads to the removal of degeneracy with respect to the orbital moment on $Mn^{+(2-\delta)}$ ions, where δ is the effective charge induced by the electron transfer from cobalt ions. The application of an external field (electric or magnetic) removes the degeneracy with respect to the direction of hybridization of the Co–Mn bonds. Cooling of the sample in an external magnetic field leads to ferromagnetic ordering of the orbitals and to the appearance of spontaneous magnetization. The concentration dependence of the normalized magnetization satisfactorily agrees with theoretical calculations using a model in which a Co^{2+} ion has only manganese ions in the nearest environment. The concentration of such clusters involving one cobalt ion and the surrounding manganese ions is $\xi = Zx(1-x)^{Z-1}$, where Z is the number of nearest neighbors in the fcc lattice ($Z = 12$). The reduced magnetization of the orbital moment in the molecular field approximation is proportional to $\sigma = M/(Ng\mu_B L) = B_L(hL\xi)$, where h is the molecular field created by the orbital moments, ξ is the concentration of these moments, and B_L is the Brillouin function with the orbital moment $L = 1$.

The ferromagnetic ordering and the formation of a spontaneous moment in $Co_xMn_{1-x}S$ solid solutions is confirmed by the hysteresis loop observed in the magnetization curve $\sigma(H)$ (Fig. 3), which disappears at $T >$ 120 K. An additional increase in the magnetization at $T =$ 15–20 K is caused by the spin–orbit splitting of electron levels on the manganese ions, the magnitude of which for Mn^{3+} amounts to $\lambda = 88$ cm^{-1} [37] and leads to an increase in the total magnetic moment. The interaction of orbitals via the lattice in the molecular field approximation can be evaluated by expanding the Brillouin function into series with respect to the exchange field h (a small parameter) in the vicinity of the temperature of formation of the spontaneous moment, which is given by the relation

$$T_c = \frac{1}{3}J_{eff}(Q)L(L+1)\xi = \frac{1}{3}L(L+1)J_{eff}(Q)Zx(1-x)^{Z-1}. \quad (3)$$

The quantity J_{eff} obeys the relation

$$J_{eff}(Q) \sim g^2(Q)/\omega(Q),$$

where $g(Q)$ is the parameter describing a change in the hopping integral caused by deformation of the lattice and $\omega(Q)$ is the phonon frequency [38]. In the proposed model, changes in the phonon frequency and in the hopping integral upon the substitution of cobalt for manganese are ignored, which implies that the parameter of interaction between the orbital moments remains constant. A change in the temperature of formation of the spontaneous moment is related only to the cobalt ions and is determined from the relation $T_c(x)/T_{c,\max} = Zx(1-x)^{Z-1}$, where $T_{c,\max}$ is the maximum critical temperature that is observed for $x = 0.05$ according to experimental data and for $x = 0.07$ according to the results of calculations. The theoretical and experimental values of the normalized temperature at which the spontaneous magnetic moment is formed are in a qualitative agreement (Fig. 10).

The application of an external electric field (Fig. 7) also removes the degeneracy with respect to the direction of hybridization of the Co–S–Mn bonds. The density of overlap of the $d_{zx} - p_z$ orbitals in the field E is $E_x \sim E\int(x^2z^2)/r^2dr$. The hopping integral increases as $t_x = E_x^2/(\varepsilon_p - \varepsilon_d)$, where ε_p and ε_d are the energies of levels for the p and d orbitals. This leads to a decrease in the resistivity since $\rho \sim 1/\sqrt{\varepsilon}$, where ε is the kinetic energy of carriers. This mechanism explains the hysteresis in the temperature dependence of the resistance measured on heating and cooling below 50 K. According to the results of calculations performed for a carrier concentration of 10^{19}, the critical voltage V_c for the onset of hysteresis in the current–voltage characteristic (Fig. 8) corresponds (with respect to the energy) to a Debye temperature of $\Theta = 240$ K, at which the orbital structure of manganese ions exhibits rearrangement.

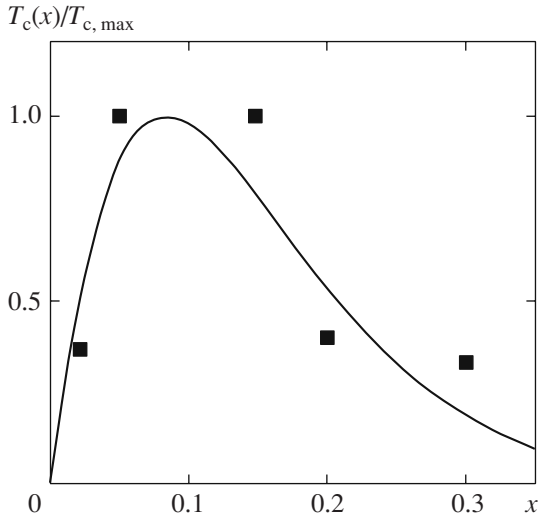

Fig. 10. Concentration dependence of the temperature of spontaneous magnetic moment formation $T_c(x)$ normalized to the maximum value $T_{c,\max}$, which is determined at $x =$ 0.05 for experimental data (points) and at $x = 0.07$ for theoretical calculations (solid curve).

5. CONCLUSIONS

We have studied the magnetic state of $Co_xMn_{1-x}S$ sulfides in the antiferromagnetic phase and determined the influence of the cobalt-ion-induced charge ordering on the transport and magnetic properties of these solid solutions. Upon the substitution of cobalt for manganese, the charge density wave exhibits pinning on the impurity levels of cobalt in the temperature intervals $\Delta T_1 =$ 200–270 K and $\Delta T_2 =$ 530–670 K. This explains the anomalous behavior of the conductivity and thermo emf observed in the indicated intervals.

A correlation between the magnetic and transport properties is established, which is confirmed by the manifestations of hysteresis in the magnetization and resistance in the same temperature interval and by the disappearance of hysteresis in the current–voltage characteristic under the action of an external magnetic field.

In the domain of magnetic ordering at temperatures below the Néel temperature (T_N), the formation of a spontaneous magnetic moment in antiferromagnetic $Co_xMn_{1-x}S$ sulfides has been observed for the first time. The appearance of a ferromagnetic orbital order in these solid solutions is related to the removal of degeneracy of the hybridized the Co–S–Mn bonds in the cubic lattice upon a decrease in the temperature. The degeneracy of the hybridized $d_{\alpha\beta}$–p_α bonds is also removed by the external electric and magnetic fields, which leads to the appearance of hysteresis.

ACKNOWLEDGMENTS

This study was supported in part jointly by the Russian and Belarusian Foundations for Basic Research (RFFI-BRFFI project no. 08-02-90031), by the Foundations for Basic Research of the Republic of Belarus (project no. F08R-037), and by the U.S. Civilian Research and Development Foundation (CRDF grant no. RUP1-1504-KR-05).

REFERENCES

1. A. V. Vedyaev, Usp. Fiz. Nauk **172** (12), 1458 (2002) [Phys. Usp. **45** (12), 1296 (2002)].
2. A. S. Borukhovich, *The Physics of Materials and Structures in Superconducting and Semiconducting Spin Electronics* (Ural Division, Russian Academy of Sciences, Yekaterinburg, 2004) p. 175 [in Russian].
3. S. Das Sarma, J. Fabian, and I. Žutic, J. Supercond. **16**, 697 (2003).
4. N. F. Mott, *Metal–Insulator Transitions* (Taylor, London, 1974; Nauka, Moscow, 1979).
5. N. Mott and E. Davis, *Electronic Processes in Non-Crystalline Materials* (Oxford University Press, Oxford, 1971; Mir, Moscow, 1982).
6. A. A. Bugaev, B. P. Zakharchenya, and F. A. Chudnovskiĭ, *The Metal–Semiconductor Phase Transition and Its Applications* (Nauka, Leningrad, 1979), p. 184 [in Russian].
7. E. L. Nagaev, *Physics of Magnetic Semiconductors* (Nauka, Moscow, 1979; Mir, Moscow, 1983).
8. E. L. Nagaev, Usp. Fiz. Nauk **166** (8), 796 (1996) [Phys. Usp. **39** (8), 637 (1996)].
9. R. V. Demin, Yu. O. Gorbenko, A. R. Kaul', et al., Fiz. Tverd. Tela (St. Petersburg) **47** (12), 2195 (2005) [Phys. Solid State **47** (12), 2287 (2005)].
10. R. V. Demin, L. I. Koroleva, A. Z. Muminov, and Ya. M. Mukovskiĭ, Fiz. Tverd. Tela (St. Petersburg) **48** (2), 305 (2006) [Phys. Solid State **48** (2), 322 (2006)].
11. G. H. Rao, L. R. Sun, J. K. Liang, et al., Appl. Phys. Lett. **69**, 424 (1996).
12. A. I. Abramovich, L. I. Koroleva, A. V. Michurin, et al., Fiz. Tverd. Tela (St. Petersburg) **42** (8), 1451 (2000) [Phys. Solid State **42** (8), 1494 (2000)].
13. Y. Shapira, S. Foner, N. F. Oliveira, et al., Phys. Rev. B: Solid State **10**, 4765 (1974).
14. A. S. Borukhovich, N. I. Ignat'eva, A. I. Galyas, et al., Pis'ma Zh. Éksp. Teor. Fiz. **84** (9), 592 (2006) [JETP Lett. **84** (9), 502 (2006)].
15. N. I. Solin and N. M. Chebotaev, Fiz. Tverd. Tela (St. Petersburg) **39** (5), 848 (1997) [Phys. Solid State **39** (5), 754 (1997)].
16. L. I. Koroleva, R. V. Demin, D. Varchevskiĭ, et al., Pis'ma Zh. Éksp. Teor. Fiz. **72** (11), 813 (2000) [JETP Lett. **72** (11), 561 (2000)].
17. Y. Zhaorong, T. Shun, C. Zhiwen, et al., Phys. Rev. B: Condens. Matter **62**, 13872 (2000).
18. P. Chen and Y. W. Du, J. Phys. Soc. Jpn. **70**, 209 (2001).
19. P. Chen and Y. W. Du, Mater. Lett. **52**, 255 (2002).
20. G. A. Petrakovskiĭ, L. I. Ryabinkina, D. A. Velikanov, et al., Fiz. Tverd. Tela (St. Petersburg) **41** (9), 1660 (1999) [Phys. Solid State **41** (9), 1520 (1999)].
21. G. A. Petrakovskiĭ, L. I. Ryabinkina, G. M. Abramova, et al., Pis'ma v Zh. Éksp. Teor. Fiz. **69** (12), 895 (1999) [JETP Lett. **69** (12), 949 (1999)]; Pis'ma Zh. Éksp. Teor. Fiz. **72** (2), 99 (2000) [JETP Lett. **72** (2), 70 (2000)].
22. G. V. Loseva, L. I. Ryabinkina, and A. A. Smyk, Fiz. Tverd. Tela (Leningrad) **28** (2), 596 (1986) [Sov. Phys. Solid State **28** (2), 334 (1986)].
23. G. A. Petrakovskiĭ, L. I. Ryabinkina, G. M. Abramova, et al., Izv. Akad. Nauk, Ser. Fiz. **66**, 856 (2002).
24. G. V. Loseva, L. I. Ryabinkina, and A. D. Balaev, Fiz. Tverd. Tela (St. Petersburg) **40** (4), 276 (1998) [Phys. Solid State **40** (4), 250 (1998)].
25. L. I. Ryabinkina, G. M. Abramova, O. B. Romanova, and N. I. Kiselev, Fiz. Tverd. Tela (St. Petersburg) **46** (6), 1038 (2004) [Phys. Solid State **46** (6), 1068 (2004)].
26. J. Goodenough, *Magnetism and the Chemical Bond* (Wiley, New York, 1963; Metallurgiya, Moscow, 1968).
27. S. S. Aplesnin, L. I. Ryabinkina, G. M. Abramova, et al., Fiz. Tverd. Tela (St. Petersburg) **46** (11), 2000 (2004) [Phys. Solid State **46** (11), 2067 (2004)].
28. R. Tappero, P. Wolfers, and A. Lichanot, Chem. Phys. Lett. **33**, 449 (2001).
29. H. H. Heikens, C. F. van Bruggen, and C. Haas, J. Phys. Chem. Soc. **39**, 833 (1978).
30. S. S. Aplesnin, L. I. Ryabinkina, G. M. Abramova, et al., Phys. Rev. B: Condens. Matter **71**, 125204 (2005).
31. D. Vaughan and J. Craig, *Mineral Chemistry of Metal Sulfides* (Cambridge University Press, Cambridge, 1978; Mir, Moscow, 1981).
32. S. Methfessel and D. Mattis, *Magnetic Semiconductors* (Springer, Heidelberg, 1968; Mir, Moscow, 1972).
33. B. I. Shklovskii and A. L. Efros, *Electronic Properties of Doped Semiconductors* (Nauka, Moscow, 1979; Springer, Berlin, 1984).
34. L. I. Ryabinkina, O. B. Romanova, G. A. Petrakovskii, et al., Phys. Met. Metallogr. **99** (Suppl. 1), S77 (2005).
35. P. Burlet, *Le titre de docteur és-sciences physiques* (De L'Université de Grenoble, Grenoble, 1968).
36. L. I. Ryabinkina, O. B. Romanova, G. A. Petrakovskiĭ, et al., in *Proceedings of the International Conference on Physics of the Solid State, Minsk, Belarus, 2005*, p. 194.
37. R. White, *Quantum Theory of Magnetism* (Springer, Heidelberg, 1983; Mir, Moscow, 1985).
38. É. L. Nagaev, *Magnetics with Complex Exchange Interactions* (Nauka, Moscow, 1988), p. 232 [in Russian].

Translated by P. Pozdeev